ELSEVIER

Carbohydrate Research 315 (1999) 16–34

CARBOHYDRATE RESEARCH

NMR study of the rotational dynamics of linear homopolysaccharides in dilute solutions as a function of linkage position and stereochemistry

Manolis Tylianakis [a], Apostolos Spyros [a], Photis Dais [a,*], Francois R. Taravel [b], Angelo Perico [c]

[a] *Department of Chemistry, University of Crete, GR-914 09 Iraklion, Crete, Greece*
[b] *Centre de Recherches sur les Macromolecules Végétales (CERMAV), CNRS, BP 53, F-38041 Grenoble, France (affiliated with the Joseph Fourier University of Grenoble)*
[c] *Instituto di Studi Chimico-Fisici di Macromolecole Sintetiche e Naturali NRC, I-16149 Genoa, Italy*

Received 9 February 1998; revised 10 July 1998; accepted 10 August 1998

Abstract

Variable temperature and magnetic field dependent ^{13}C NMR relaxation measurements (T_1, T_2, and NOE) were carried out on a series of linear homopolysaccharides: α-(1→3)-D-glucan, β-(1→3)-D-glucan in Me_2SO-d_6, and α-(1→6)-D-glucan in D_2O and Me_2SO-d_6 dilute solutions. The relaxation data of the backbone carbons were analyzed quantitatively by using a variety of theoretical unimodal and bimodal time-correlation functions in an attempt to describe the main carbohydrate chain dynamics as a function of linkage position and stereochemistry. Among these, the time-correlation function developed by Dejean, Laupretre, and Monnerie (DLM) offered the best quantitative description of the segmental motion of the carbohydrate chains. The internal rotation of the hydroxymethyl groups about the exocyclic C-5–C-6 bonds superimposed on segmental motion has been described as a diffusion process of restricted amplitude. Comparison of the dynamics of polysaccharides has been extended to include amylose and inulin studied previously. On the basis of the calculated correlation times for segmental motion, the flexibility of the carbohydrate chains decreases from inulin and dextran following the order; inulin > dextran > α-(1→3)-D-glucan > β-(1→3)-D-glucan ~ amylose, whereas the rate and the amplitude of the internal rotation of the hydroxymethyl groups about the exocyclic C-5–C-6 bonds showed that the restriction of the hydroxymethyl internal rotation decreases from inulin to amylose following the order; inulin > α-(1→3)-D-glucan ~ β-(1→3)-D-glucan > amylose. Solvent effects on segmental dynamics and the temperature–frequency superposition of the relaxation data of the three polysaccharides have been discussed as well.

Keywords: NMR-relaxation; Polysaccharides; Dynamics; Time-correlation functions

1. Introduction

The ubiquity and the diversity of carbohydrate polymers like cellulosics, starches, alginates, and various types of gums (e.g., agar, guar, arabic, etc.) in nature is well known. Their industrial uses have been widened to control the rheology of the aqueous phase, as thickeners, suspending and/or gelling agents, as well as systems with intermediate properties [1]. Moreover, polysaccharide molecules serve as storage materials, such as starch, and as structural materials in plants (cellulose) and in the exoskeletons of insects (chitin).

* Corresponding author. Tel.: +30-81-238-468; fax: +30-81-219-851.

0008-6215/99/$ - see front matter
PII: S0008-6215(98)00263-8

Carbohydrate polymers are superbly effective carriers of information in cell recognition. Surface polysaccharides on a cell serve as points of attachment for other cells, infectious bacteria, viruses, toxins, hormones and many other molecules. In this way carbohydrate polymers, chemically linked to proteins (glycoproteins), or to fats (glycolipids), mediate the migration of cells during embryo development, the process of infection and other phenomena [2]. In addition to the carbohydrate-directed interactions between cells, which are related to pathological phenomena, carbohydrate molecules are also crucially important to the healthy operation of the immune system, and the defense against the spread of cancer cells from the main tumor throughout the human body [3].

Such a diversity of properties is undoubtedly the result of different chemical structures of the polysaccharide chains. In part, this is due to the different nature of the monomer residues that constitute the polymeric chain, and in part, due to the type of linkages that connect residues in the chain. For instance, many of the 12 pyranoside monosaccharides of the D-series can be found in polysaccharides. Furthermore, these monomers are connected by $1\rightarrow2$, $1\rightarrow3$, $1\rightarrow4$ (and $1\rightarrow6$ in the case of hexoses) linkages, and each type of linkage exists in the α or β anomeric configuration. Considering that these sugar residues and linkages could occur in various combinations, as linear copolymers and branched polysaccharides, the total number of possible structures is enormous.

In the past, many experimental and theoretical studies attempted to correlate the properties of the various polysaccharides with their chemical structures, conformations [4–12], and complete three-dimensional structures [13–16] with remarkable success. For instance, Rees and Scott [4] attempted to classify the physical structure and the ranges of stereochemically-allowed conformations of a number of linear polysaccharides by employing a simple model of conformational analysis. Nevertheless, little effort has been devoted to exploring the influence of the conformational dynamics of polysaccharides in solution on structure–properties relationship [17–22]. Little is known about possible correlations between linkage type, and/or sugar monomer and the rate or dynamics of conformational change. Several studies [23–26] employ ^{13}C NMR relaxation measurements, and analyze the experimental data in qualitative or semiquantitative terms, whereas only a few investigations [27–32] have attempted to describe the dynamics of polysaccharides by using explicit dynamic models. Although qualitative analysis of ^{13}C relaxation data appears to be useful for spectral assignments and for describing the gross features of flexibility, it is likely to be less valuable than quantitative information inherent in the measured ^{13}C relaxation parameters. The analysis of the multi-field relaxation data of amylose [27–29,31], dextran [27], inulin [31], and sodium pectate [32] shows how complex the dynamics of carbohydrate chains can be.

In this paper, we address the issue of structure–properties relationship by employing ^{13}C NMR relaxation experiments to study and compare the conformational dynamics of three linear polysaccharides that differ in the linkage type, namely, α-(1→3)-D-, β-(1→3)-D-, and α-(1→6)-D-linked glucans. The comparison will be extended to include the α-(1→4)-D-glucan (amylose), and β-(2→1)-linked fructofuranosyl residues of inulin that have been studied earlier [31]. Representative dimeric segments of α-(1→3)-D-, β-(1→3)-D-, and α-(1→6)-D-glucans are shown in Fig. 1.

2. Experimental

Materials.—β-(1→3)-D-glucan was purchased from Takeda Chemical Industries (Japan). Dextran was obtained from Pharmacia Fine Chemicals. α-(1→3)-D-glucan was produced by *Streptococcus mutans* bacteria, and was a gift from Dr H. Chanzy (CERMAV, Grenoble) and Dr K. Ogawa (Japan). Weight-average molecular weights, M_W, were determined by light scattering and are summarized in Table 1. Table 1 also contains the molecular weights of amylose and inulin determined previously [29,31].

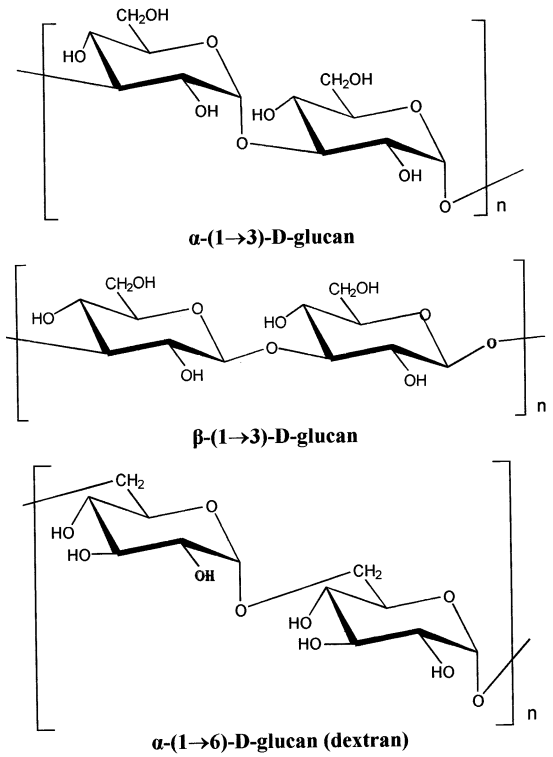

Fig. 1. Structures of polysaccharides.

NMR relaxation.—^{13}C NMR relaxation measurements were conducted at three ^{13}C Larmor frequencies, (75.4, 100.5 and 125.7 MHz) on Bruker AC300, AM400, and Varian Unity 500 spectrometers, respectively, under broadband proton decoupling. Temperature was controlled to within ± 1 °C by means of precalibrated thermocouples in the probe inserts. Calibration was achieved by using ethylene glycol samples.

Spin-lattice relaxation times (T_1) were measured by the standard IRFT method with a repetition time longer than $5T_1$. A total of 256–640 transients were accumulated, for a set of 8–12 arrayed τ values, depending on the type of spectrometer and temperature. The 180° pulse width ranged from 27 to 29 μs in the three spectrometers. Values of T_1 were determined by a three-parameter nonlinear procedure with an rms error of $\pm 10\%$, or better. The reproducibility of each T_1 value was $\pm 5\%$. Measurements of spin–spin relaxation times (T_2) were performed by using the Carr–Purcell–Meiboom–Gill (CPMG) pulse sequence with complete broadband decoupling of protons. However, to avoid an irreversible diminution in the measured T_2 values as compared to the true values [33], decoupling was switched off during echo formation, but reestablished during acquisition and over a long delay time ($\sim 5T_1$) before the repetition of the pulse sequence. The duration of the 180° pulse train covered a range of 2 ms up to 4–5 times the longest T_2 value. The accuracy of the measured T_2 values was estimated to be ± 15–20%. NOE experiments were carried out by inverse gated decoupling, at least three experiments being performed at each temperature value. Delays of at least 10 times the longest T_1 were used between 90° pulses. NOE values were estimated to be accurate to within $\pm 15\%$.

Undegassed samples of polysaccharides in Me_2SO and water solutions (5–10% w/v, depending on solubility) were used for the ^{13}C relaxation experiments. Measurements with degassed samples did not show any measur-

Table 1
Molecular weights, intrinsic viscosities (mL g^{-1}), Huggins constants and molecular correlation times of the overall motion of the various polysaccharides

Polysaccharide	Solvent	$M_W \times 10^3$	$[\eta]^a$	k'	$\tau_R(\times 10^{-7})$
Amylose[b]	(Me_2SO-d_6)	330	104.7	0.414	7
Dextran	(Me_2SO-d_6)	35	68.6	2.512	143.6
	(D_2O)		46.1	2.525	3.6
α-(1→3)-D-glucan	(Me_2SO-d_6)	7.5	50.0	2.128	2
β-(1→3)-D-glucan	(Me_2SO-d_6)	400	502.8	3.11	105
Inulin[b]	(D_2O)	5.5	17		0.2

[a] At 30 °C in the appropriate solvents.
[b] Refs. [27,29].

able difference in the ^{13}C relaxation parameters relative to those of the undegassed samples, in agreement with earlier reports [31,34,35] in polymeric systems that show relaxation parameters on the millisecond timescale. Also, change of concentration from 5 to 10% w/v, where possible, did not show any appreciable difference in the ^{13}C relaxation parameters. Concentration-independent relaxation parameters from 5–15% w/v have been observed in many synthetic polymers [35].

COSY.—The gradient-selected H, H-COSY spectrum [36] of dextran was obtained using 64 increments of 4K real data points with 512 transients for each free induction decay, and a recycle delay of 1.5 s. Before Fourier transformation the data set was zero-filled to a $4 \times 4K$ matrix. Sinebell weighting functions were applied in both dimensions.

HSQC.—The phase-sensitive gradient-selected hydrogen–carbon heteronuclear single quantum coherence [36] experiment in this work was acquired with 1024 transients and 256 increments of 2K. The relaxation delay was 2 s. Zero-filling to $4 \times 4K$ and sine multiplication were performed prior to Fourier transformation.

Viscosity.—Viscosity measurements were performed using Ubbelohde-type dilution viscometers in a bath thermostatted at 30 ± 0.01 °C. Intrinsic viscosities, $[\eta]$, and Huggins constants, k', were calculated through Eq. (1) by plotting η_{sp}/C vs C:

$$\eta_{sp}/C = [\eta] + k'[\eta]^2 C \quad (1)$$

where η_{sp} is the specific viscosity. These values are tabulated in Table 1.

Molecular weights.—The molecular weights of the various polysaccharides used in the present study were determined at 25 °C through static and dynamic light scattering measurements using a ALV/DLS-5000 laser system. Solutions in Me_2SO solvent were used.

Numerical calculations.—The relaxation data were analyzed by using the MOLDYN program [37], modified to include the spectral density functions used in the present study. Details of the program and fitting procedures by employing various models have been given elsewhere [29,37].

3. Results and discussion

Frequency and temperature dependence of the ^{13}C NMR relaxation data.—The variable temperature, multifield ^{13}C NT_1, NT_2 (N is the number of directly attached protons to carbons), and NOE values for the ring carbons and the exocyclic hydroxymethyl carbons of dextran in water and Me_2SO, and of β-(1→3)-D-glucan in Me_2SO are shown in Figs. 2 and 3, respectively, over the whole temperature range studied at three magnetic fields (75.4, 100.5, and 125.7 MHz). Figs. 2(a,b) and 3(a,b) depict the NT_1 and NOE values for the ring carbons and the exocyclic hydroxymethyl carbons of α-(1→3)-D-glucan in Me_2SO, respectively, at two magnetic fields (75.4 and 100.5 MHz), and the NT_2 parameter at one magnetic field (125.7 MHz).

For α- and β-(1→3)-D-glucans in Me_2SO, the relaxation parameters of the ring carbons were similar within experimental error, and hence the average values are shown in Figs. 2(a,b) and 2(c,d), respectively. For the same reason, average values for the relaxation parameters of the ring carbons of dextran in Me_2SO are shown in Fig. 2(e,f). However, the relaxation parameters for the C-4 carbon of the same polysaccharide in water were different from the corresponding values of the remaining ring carbons, and therefore, they are depicted separately in Fig. 2(g,h), whereas the average relaxation parameters of the remaining ring carbons are shown in Fig. 2(i,j).

Inspection of Fig. 2(a–j) for the relaxation parameters of the ring carbons reveals a number of motional characteristics that are commonly observed in the ^{13}C relaxation data of most polymeric materials [23,34,35]: (1) as the temperature decreases the NT_1 values decrease monotonically, at all fields, reaching a minimum, which is followed by an increase in NT_1 with further decrease in temperature; (2) the minimum is shifted to higher temperatures (shorter correlation times) as the magnetic field increases; (3) at a given temperature and solvent, NT_1 values increase with increasing magnetic field, the difference in NT_1 values among the magnetic fields becoming more pronounced as the temperature decreases

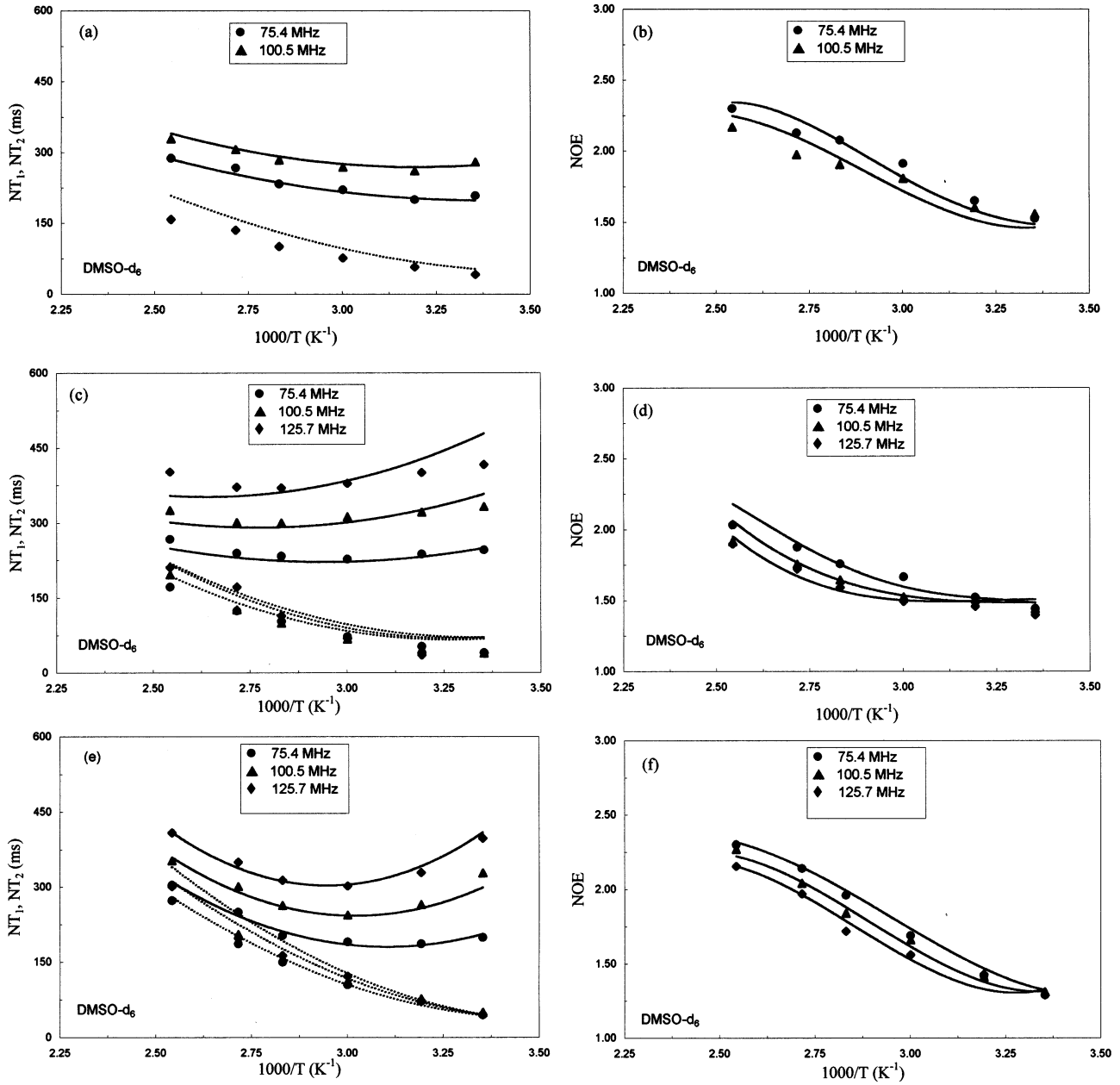

Fig. 2. Temperature dependence of the experimental and calculated relaxation data for the ring carbons of polysaccharides at magnetic fields (●) 75.4, (▲) 100.5, and (◆) 125.7 MHz. For α-(1→3)-D-glucan in Me_2SO-d_6 (a) NT_1, NT_2, (b) NOE; for β-(1→3)-D-glucan in Me_2SO-d_6 (c) NT_1, NT_2, (d) NOE. For dextran in Me_2SO-d_6 (e) NT_1, NT_2, (f) NOE. For the C-4 carbon of dextran in D_2O (g) NT_1, NT_2, (h) NOE. For the C-1, C-2, C-3, and C-5 carbons of dextran in D_2O; (i) NT_1, NT_2, (j). Solid curves correspond to the DLM model fitting of NT_1 and NOE values. Dashed curves corresponds to the DLM fitting of the NT_2 values.

(slow motion regime); (4) the NT_2 values decrease continually with decreasing temperature, and they are always much smaller than NT_1 values, especially at low temperatures; (5) the NOE values decrease with increasing magnetic field, although they tend to converge as temperature decreases, reaching the slow motion regime; (6) at high temperatures, where motions become faster, NOE values are less than the theoretical maximum of 2.988.

These experimental observations preclude the possibility of describing the dynamics of these polysaccharides using a single exponential time correlation function (TCF) [23,31,34,35]. The same trends are observed for the relaxation behavior of the exocyclic

hydroxymethyl groups in Fig. 3(a–h), although the T_1 minima in these curves are shifted to higher temperatures relative to those of the ring carbons at the same field, indicating that these exocyclic carbons are more mobile than the ring carbons. This conclusion is supported by the higher NOE values observed for the hydroxymethyl carbons relative to the NOE values of the ring carbons (for instance, compare Figs. 2(b) and 3(b)). However, even for these mobile groups the NOE values are less than 2.988. Comparing the NMR relaxation data of dextran (Fig. 2(e,f)) and the two α- and β-(1→3)-D-glucans (Figs 2(a,b) and 2(c,d)) in the same Me_2SO solvent, we make the following observations: (1) the minimum of the NT_1 values for the ring carbons of dextran is shifted to lower temperatures relative to that of the two glucans; (2) the NOE values for the ring carbons of dextran are higher than those of the two glucans. These observations indicate that the dextran chain is characterized by a greater flexibility than the chains of the two glucans.

The opposite behavior is observed for the minimum of the NT_1 values of the hydroxymethyl carbons of these polysaccharides. The minimum of the NT_1 values for dextran in Me_2SO (Fig. 3(e)) are shifted to higher temperatures than the corresponding minima of the two glucans in the same solvent (Figs. 3(a) and (c)), indicating a faster internal rotation of the exocyclic hydroxymethyl groups in the two glucans than in dextran. This observation is not surprising, since the position of the hydroxymethyl group of dextran on the polymer backbone, as part of the (1→6)-D-glucosidic linkage, appears to induce a greater steric hindrance to its internal motion relative to that of each hydroxymethyl methyl group in the two glucans. The latter two groups are attached to the backbones of the two glucans by single bonds.

Another interesting observation from the data is that the ratio of the NT_1 values of the C-4 carbon to the NT_1 values of the remaining ring carbons, NT_1(C-4)/NT_1(C-1–C-5), for dextran in water is fairly constant at 0.91 ±

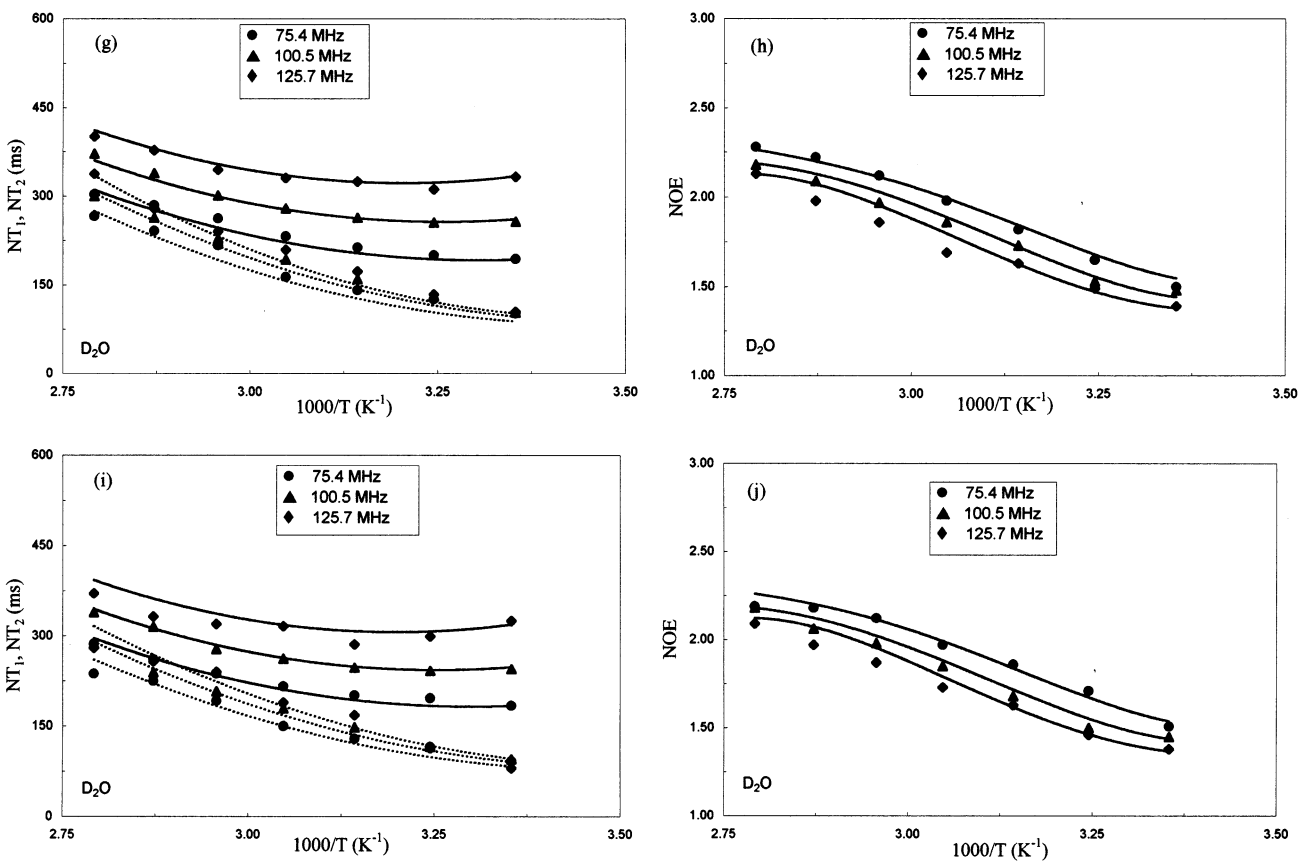

Fig. 2. (*Continued*)

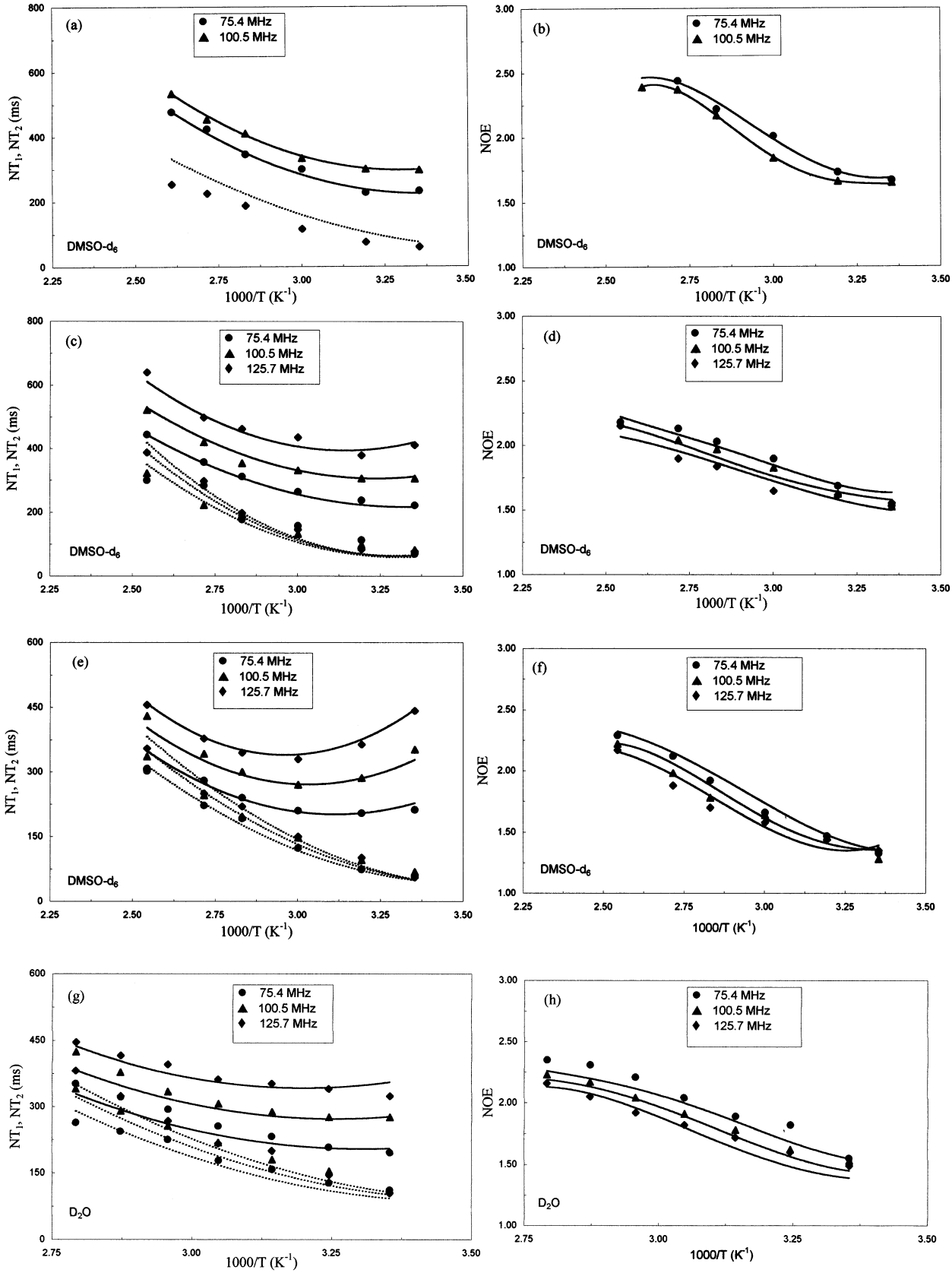

Fig. 3. Temperature dependence of the experimental and calculated relaxation data for the hydroxymethyl carbons of polysaccharides at magnetic fields (●) 75.4, (▲) 100.5, and (◆) 125.7 MHz. For α-(1→3)-D-glucan in Me_2SO-d_6 (a) NT_1, NT_2, (b) NOE. For β-(1→3)-D-glucan in Me_2SO-d_6 (c) NT_1, NT_2, (d) NOE. NOE. Solid curves correspond to the restricted diffusion model fitting of NT_1 and NOE values. Dashed curves correspond to the restricted diffusion model fitting of the NT_2 values. For dextran in Me_2SO-d_6 (e) NT_1, NT_2, (f) NOE. For dextran in D_2O (g) NT_1, NT_2, (h) NOE. Solid curves correspond to the DLM model fitting of NT_1 and NOE values. Dashed curves corresponds to the DLM fitting of the NT_2 values.

0.05 at all fields throughout the temperature range studied. This value differs from the value of 1, which is expected from the number of directly bonded protons, and suggests different local motions for the C–H internuclear vectors associated with the C-4 and the remaining ring carbons. This differential in the local dynamics of the ring C–H vectors of polysaccharides has been observed previously in amylose and inulin [31].

Modeling the dynamics of polysaccharides.—In modeling the dynamics of polysaccharides, two types of motions are considered: First the overall rotatory diffusion of the carbohydrate chain as a whole and second, local chain motions. Local chain motions in a carbohydrate chain are considered to be: (1) the oscillatory motions about the glycosidic bonds, which represent the so-called segmental motions; (2) internal motions of substituents attached to the carbohydrate chain via chemical bonds, such as methyl, or hydroxymethyl groups; (3) a third type of very fast local motion (about 10^{-11} s), which usually occurs in synthetic polymers, may be the small-amplitude librations of particular backbone C–H vectors within a potential well. As we shall see later, these motions are strongly affected by the local geometry of the carbohydrate chain. Each of these motions is considered as an independent source of motional modulation of the $^{13}C-^{1}H$ dipole–dipole interactions for the protonated carbons of the polysaccharides. Since the time-correlation function, $G_0(t)$, of the overall motion for a polymer chain of high molecular weight is a slowly decaying function (correlation time 10^{-5}–10^{-8} s), and the TCF, $G_1(t)$, for the local motions is a faster decaying function (correlation time 10^{-9}–10^{-11} s), these two motions can be considered as independent [23,29]. Accordingly, their respective TCFs can be safely separated in the total TCF, $G(t)$, that is:

$$G(t) = G_0(t)G_1(t) \tag{2}$$

As we shall see later, the time scales of the various local motions in the present polysaccharide chains differ by one to two orders of magnitude, and therefore the decoupling of their TCFs is considered a good approximation.

Overall rotatory diffusion.—For sufficiently high molecular weight random coil polymers (above a critical value of 1000–10,000 depending on chemical structure), the overall motion is much slower than the chain local motions, and thus makes a negligible contribution to the T_1 values of the backbone and side-chain carbons [23,34,35]. The molecular weight of the present polysaccharide molecules lies above this limit. Our neglect of the overall motion is further supported by estimations of the overall motion correlation time, τ_R. Since the correlation time of the overall motion cannot be determined from relaxation data alone (all carbons in the carbohydrate chain relax via both the overall and local motions), this parameter must be simulated by using the hydrodynamic equation, which holds for infinite dilution [38]:

$$\tau_{R'} = \frac{2M_W[\eta]\eta_0}{3RT} \tag{3}$$

where M_W is the molecular weight, $[\eta]$ is the intrinsic viscosity of the polymer solution and η_0 is the solvent viscosity. In a solution of finite concentration, c, the correlation time, τ_R, is estimated from the following equation [29,39]:

$$\ln(\tau_R/\tau'_R) = k'[\eta]c \tag{4}$$

where k' is the Huggins constant (Eq. (1)). The calculated τ_R values for the three polysaccharides are summarized in Table 1. The results reported here should represent polysaccharide behavior in the high molecular weight limit. The reported relaxation parameters are therefore dominated by local polymer dynamics.

Segmental motions.—In polymers, the dominant relaxation process is the $^{13}C-^{1}H$ dipolar interactions [40]. Also, for these systems, only interactions with directly bonded protons need be considered. Under conditions of complete proton decoupling the ^{13}C relaxation parameters, T_1, T_2, and NOE can be written in terms of the spectral density function, $J_i(\omega_i)$, as follows (in the SI system) [41]:

$$\frac{1}{T_1^{DD}} = \frac{\Omega}{10}[J_0(\omega_H - \omega_C) + 3J_1(\omega_C) + 6J_2(\omega_H + \omega_C)] \tag{5}$$

$$\frac{1}{T_2^{DD}} = \frac{1}{2T_1^{DD}} + \frac{\Omega}{20}[4J(0) + 6J_1(\omega_H)] \quad (6)$$

$$NOE = 1 + \frac{\gamma_H}{\gamma_C}\frac{\Omega T_1}{10}[6J_2(\omega_H + \omega_C) - J_0(\omega_H - \omega_C)] \text{ and } \Omega = N\left(\frac{\mu_0\gamma_H\gamma_C h}{8\pi^2 r_{CH}^3}\right)^2 \quad (7)$$

where γ_H and γ_C are the gyromagnetic ratios of proton and carbon nuclei, respectively, ω_H, ω_C are their Larmor frequencies, μ_0 is the vacuum magnetic permeability, h is Planck's constant, N is the number of directly bonded protons, and r_{CH} is the C–H internuclear distance. The spectral density function required for the calculation of the relaxation parameters by means of Eqs. (5)–(7) should be obtained upon Fourier transform of the appropriate time-correlation function:

$$J_m(t) = 2\mathrm{Re}\left[\int_0^{\infty} G_m(\omega)e^{i\omega t}\,dt\right] \quad (8)$$

with Re indicating the real part of the complex Fourier transform.

Several attempts [23,27,30–32] have been made in the past to interpret the relaxation of polysaccharides in solution by employing a variety of theoretical TCFs suitable for local chain motions of synthetic polymers [34,35]. For synthetic polymers, there is a general consensus [34,42] that bimodal TCFs, such as the modified $\log(\chi^2)$ distribution [43], and the model [44], are better models than unimodal TCFs, such as the original $\log(\chi^2)$ model proposed by Schafer [45], the conformational model developed by Hall–Weber–Helfand [46] (HWH model), and the diamond-lattice Dejean–Laupretre–Monnerie (DLM) model described by Jones–Stockmayer [47] (JS model). The ability of the various models to describe the dynamics of the segmental motions of polysaccharides in solutions has been tested in a previous publication on amylose and inulin [31]. The DLM time-correlation function offered a much better description of the segmental dynamics of these biopolymers.

Application of all unimodal TCFs failed to reproduce the experimental relaxation parameters NT_1, NT_2, and NOE at the minimum of the curves of NT_1 as a function of temperature and magnetic field of the present polysaccharides. Therefore, the DLM model and the modified $\log(\chi^2)$ distribution will be used in the following analysis. The DLM model is an effective modification of the HWH model to account for different local dynamics observed experimentally at different carbon sites in the chain. The DLM time-correlation function describes the backbone reorientation in terms of two motional processes [44,46]: (1) a diffusion process along the chain, which, according to the HWH model, occurs via conformational transitions described by two correlation times τ_0 and τ_1, for isolated, single-bond conformational transitions and for cooperative transitions, respectively, (2) bond librations, i.e., wobbling in a cone motion of the backbone internuclear C–H vectors as described by Howarth [48]. The librational motion is associated with a correlation time τ_2, whereas the extent of the libration about the rest position of the C–H bond, which coincides with the axis of the cone is determined by the cone, half-angle, θ. The DLM spectral density function is given explicitly in Ref. [44].

The TCF of the modified $\log(\chi^2)$ distribution can be expressed by a distribution of correlation times, which involves librational motions of the backbone C–H vectors. The parameters of this model are the width of the distribution, p, and the average correlation time, τ, characterizing the center of the distribution. The librations are represented by a delta function with correlation time τ_2. The extent of the librations inside the cone is described as before by the cone half-angle θ. The explicit TCF of this model can be found in Ref. [43].

The modified (bimodal) $\log(\chi^2)$ model was successful in reproducing the relaxation data of α-(1→3)-, and β-(1→3)-glucans, but not those of the polysaccharide dextran in Me_2SO and water solutions. In contrast, the DLM model provides an excellent fit between experimental and calculated NT_1, NT_2, and NOE data for all the ring carbons of the three polysaccharides at the various magnetic fields. The reason why the DLM function works for all the polysaccharides, while the modified $\log(\chi^2)$ model does not, may be attributed to the very different shape of their respective

TCFs [42,44]. The shape of the modified $\log(\chi^2)$ distribution, which describes the segmental motion, makes this model ineffective in lifting up the minimum NT_1 as the width of the distribution decreases. Since dextran is a more flexible polysaccharide than the other two glucans, the distribution of the correlation times is expected to be narrower in the former polysaccharide than in the latter biopolymers.

The best fit NT_1, NT_2, and NOE data as a function of temperature and magnetic field for the ring carbons of the three polysaccharides, are shown graphically in Fig. 2(a–j), by employing the DLM model. It is seen from these plots that good agreement between experimental and calculated values is obtained from this model throughout the entire temperature range studied. In all cases, the percentage differences between the experimental and calculated values were within the experimental error ($\pm 10\%$) of the relaxation measurements. For this model, the values of the fitting parameters are summarized in Table 2. Table 2 also contains the fitting parameters of the DLM model for amylose and inulin taken from a previous study [31].

The simulated values for the angles θ of the ring carbons of α-(1→3)- and β-(1→3)-glucans, dextran in Me_2SO, and the C-1, C-2, C-3, and C-5 carbons of dextran in water are similar (Table 2). The average value of about 29° indicates the same local dynamics at these carbon sites for the three polysaccharides. The τ_1 values derived from fitting the experimental relaxation data for the ring carbons of the three polysaccharides with the DLM model

Table 2
Correlation times (10^{-10} s), librational angles ($\theta°$), diffusional angle ($\chi°$), and activation energies (kJ mol^{-1}) obtained from the DLM and restricted diffusion TCFs for the polysaccharides amylose[a,b], dextran[a,c], α-(1→3)-D-glucan[a], β-(1→3)-D-glucan[a], and inulin[b,c]

	Amylose			Dextran		α-(1→3)-D-glucan			β-(1→3)-D-glucan			Inulin		
t (°C)	τ_1	τ_i	$\chi°$	τ_1[a]	τ_1[c]	τ_1	τ_i	$\chi°$	τ_1	τ_i	$\chi°$	τ_1	τ_i	$\chi°$
25	45.73	0.67	37	36.88	14.96	42.74	0.52	57	42.34	0.64	39	17.54	0.42	62
35					11.15							13.82	0.34	71
40	39.28	0.54	39	17.91		22.09	0.37	55	32.31	0.64	48			
45					7.45							10.85	0.28	81
55					5.35							7.92	0.25	93
60	24.38	0.45	46	9.64		13.61	0.22	59	21.35	0.34	59			
65					3.46							5.91	0.21	107
75					2.49							4.47	0.20	102
80	14.13	0.32	52	6.26		7.45	0.20	69	14.19	0.26	68			
85					2.03							3.41	0.13	135
95						4.82	0.17	82	9.35	0.18	72			
100	9.28	0.20	55	3.91										
110														
120	5.85	0.18	57	2.26		3.37	0.12	77	4.63	0.10	74			
τ_0/τ_1	7			3	8	3			5			2		
τ_1/τ_2	100			200	140	30			100			90		
θ (C-1)	21.5													
θ (C-3)												26		
θ (C-4)					24							29		
θ (C-5)												33		
θ (C-6)														
θ (C-ave)	27			28.5	28	28.5			29.5					
E_a	22	14		28	31	27.5	14		22	18		25	16	
r	0.99	0.97		0.99	0.99	0.98	0.97		0.99	0.97		0.99	0.98	

[a] In Me_2SO-d_6.
[b] Ref. [29].
[c] In D_2O.

are compiled in Table 2. These values indicate that the segmental motion of dextran is about 1.5 times faster than that of α-(1→3)-D-glucan, and 2–2.5 times faster than that of β-(1→3)-D-glucan in Me_2SO at all temperatures, except perhaps at 25 °C. This provides direct evidence of the greater flexibility of the dextran chain relative to the flexibility of the chains of the other two glucans. From Fig. 1, which shows the structures of the three polysaccharides, one can conclude that the C-1–O-1–C-6–C-5 glycosidic bond connecting the two adjacent D-glucopyranosyl rings in dextran offers somewhat greater motional freedom than the simple C–O–C bond connecting the rings in α-(1→3)-D- and β-(1→3)-D-glucans.

Comparison of the τ_1 values of dextran in water and Me_2SO solutions shows that this polysaccharide is more flexible in water than in Me_2SO by a factor of 2. However, this comparison does not separate solvent effects that are not implicit in the DLM model. Assuming that solvent effects can be represented by solvent viscosity, we divide the correlation times by the solvent viscosity at each temperature. The corrected τ_1 values do not show any appreciable difference in the mobility of dextran in the two solvents.

Plots of the logarithms of these values as a function of $1/T$ (K) show linear correlations, in the temperature range studied, yielding apparent activation energies, E_a, of 28 and 31 kJ mol^{-1} for dextran in Me_2SO and water solutions, respectively, 27.5 kJ mol^{-1} for α-(1→3)-D-glucan and 22 kJ mol^{-1} for β-(1→3)-D-glucan in Me_2SO solutions. The potential barrier, E^*, of the conformational transitions associated with the τ_1 correlation time can be estimated from the equation:

$$E^* = E_a - E_\eta \quad (9)$$

assuming that Kramers theory [49] at the high friction limit is valid for these polysaccharides. E_η is the activation energy for the viscous flow, and is 13 kJ mol^{-1} for Me_2SO and 15 kJ mol^{-1} for water [31]. This leads to values of barrier heights E^* of 15 and 16 kJ mol^{-1} for dextran in Me_2SO and water solutions, respectively, 14.5 kJ mol^{-1} for α-(1→3)-D-glucan, and 9 kJ mol^{-1} for β-(1→3)-D-glucan in Me_2SO solutions. These values are similar to those obtained for synthetic polymers [34,35] and other polysaccharides in solutions [31].

The different local dynamics at the C-4 carbon as compared to that of the remaining ring carbons of dextran in water, discussed previously, is reflected on the calculated θ values, which are 24° for the C-4–H-4 vector and 28° on average for the remaining C–H vectors. This trend in the θ values in dextran, which is unique among the three polysaccharides, reflects the different magnitude of the steric hindrance to the librational motion at the C-4 carbon site of dextran. The origin of the observed differentials in the librational angle at position C-4 of dextran in water relative to that in Me_2SO could be the formation of intramolecular hydrogen-bonding. X-ray diffraction studies [50] and theoretical calculations [51] have shown the existence of O-2–O-4′ hydrogen-bonding between adjacent glucose residues. This hydrogen-bonding may persist in water, but not in Me_2SO solutions. It has been suggested [52] that in the latter solvent, each hydroxyl group tends to form intermolecular hydrogen-bonds with the solvent molecules. Another possibility may be the formation of a hydrogen bonding network among the three hydroxyl groups of the glucopyranosyl ring of dextran. In both cases, all carbon sites could show the same local dynamics in Me_2SO solutions, but not in D_2O solutions.

To check this possibility, we recorded ^1H NMR spectra of dextran in Me_2SO as a function of temperature, and studied the temperature-dependence of the hydroxyl chemical shifts. The resonances of the protons of the hydroxyl groups, which are hydrogen-bonded to the solvent, migrate upfield with increasing temperature and show a substantial temperature coefficient ($d\delta/dT$), whereas intramolecular association should be manifested by a relative insensitivity of the proton chemical shift to temperature [52,53]. When $d\delta/dT \approx 0$, the proton in question is considered to form an intramolecular hydrogen bond. However, there are problems of interpretation when $d\delta/dT$ is negative or greater than a reference value. For the latter situation, it has been suggested [52,54] that differentiation may be

made on the basis that intramolecularly hydrogen-bonded protons show the least temperature dependence.

The chemical shifts of the ring and hydroxyl protons of dextran in Me_2SO have been determined by employing 2D NMR experiments. The ring proton resonances were determined on the basis of the known ^{13}C chemical shifts of dextran [55] through an HSQC experiment at 30 °C. The ^1H NMR spectrum in one dimension does not show hydroxyl signals, since their respective protons have been exchanged by deuterium nuclei in D_2O solution. The hydroxyl proton peaks were connected to the ring proton resonances by performing a H, H-COSY experiment. The 2D NMR spectra and the assignment of the ring and hydroxyl protons are shown in Figs. 4 and 5. Fig. 6 illustrates the variation of the chemical shifts of the three hydroxyl protons with temperature. For all hydroxyl protons, the temperature dependence of the chemical shifts is negative and the slopes, $d\delta/dT$, of the straight lines are very close to zero (-0.005 for OH-4, -0.006 for OH-3, and -0.007 for OH-2). This observation indicates that the three hydroxyl groups form an intramolecular hydrogen-bonding network in Me_2SO solutions.

Hydroxymethyl internal rotation.—A number of models exist in the literature describing internal mobility as a free rotation, restricted rotation about a bond, a wobbling motion in which a vector diffuses within a cone, or jumps between equivalent, or nonequivalent states. An extensive discussion of these models can be found in Refs. [23,29,34,35].

The internal motion of the hydroxymethyl groups of α-(1→3)-D-, and β-(1→3)-D-glucans about the exocyclic C-5–C-6 bonds superimposed on segmental motion could not be described by assuming free rotation of 360° about this bond. Composite TCFs [39,56] based on the HWH model and the Woessner equations [57] for stochastic diffusion and jump processes did not reproduce the experimental data for the C-6 carbon of amylose and inulin. For this reason, TCFs describing restricted internal motions should be used in

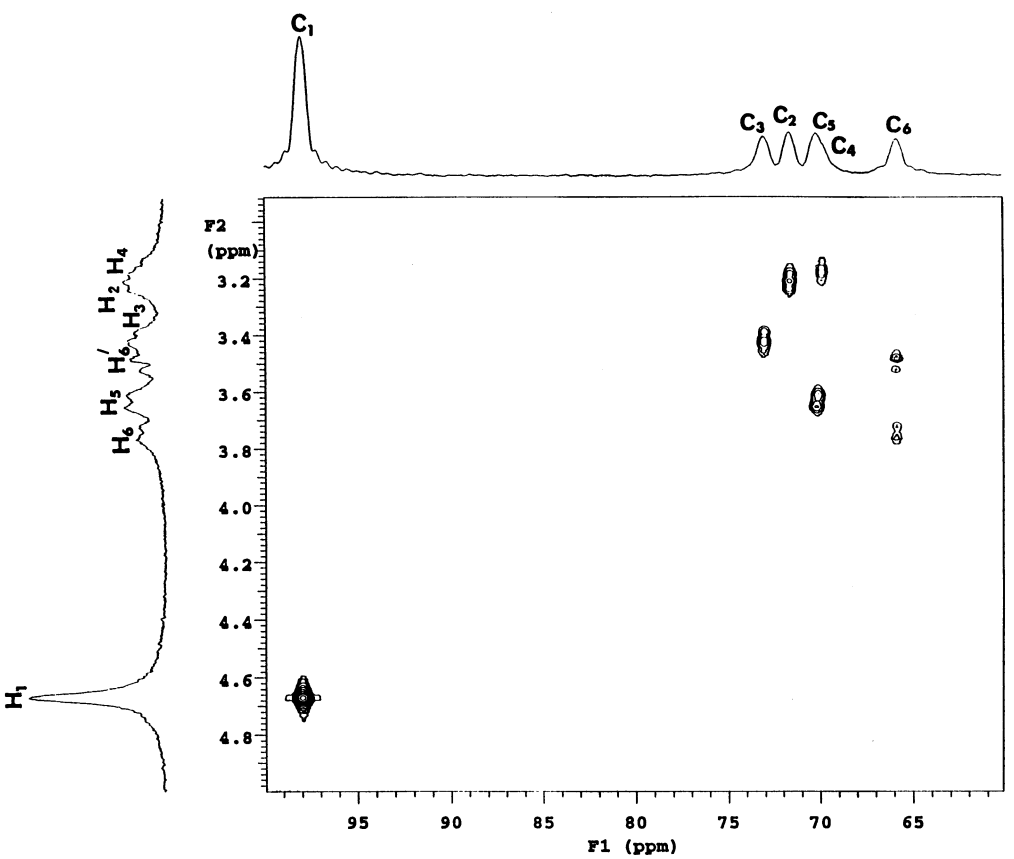

Fig. 4. Gradient HSQC spectrum of dextran in Me_2SO-d_6 solutions at 30 °C.

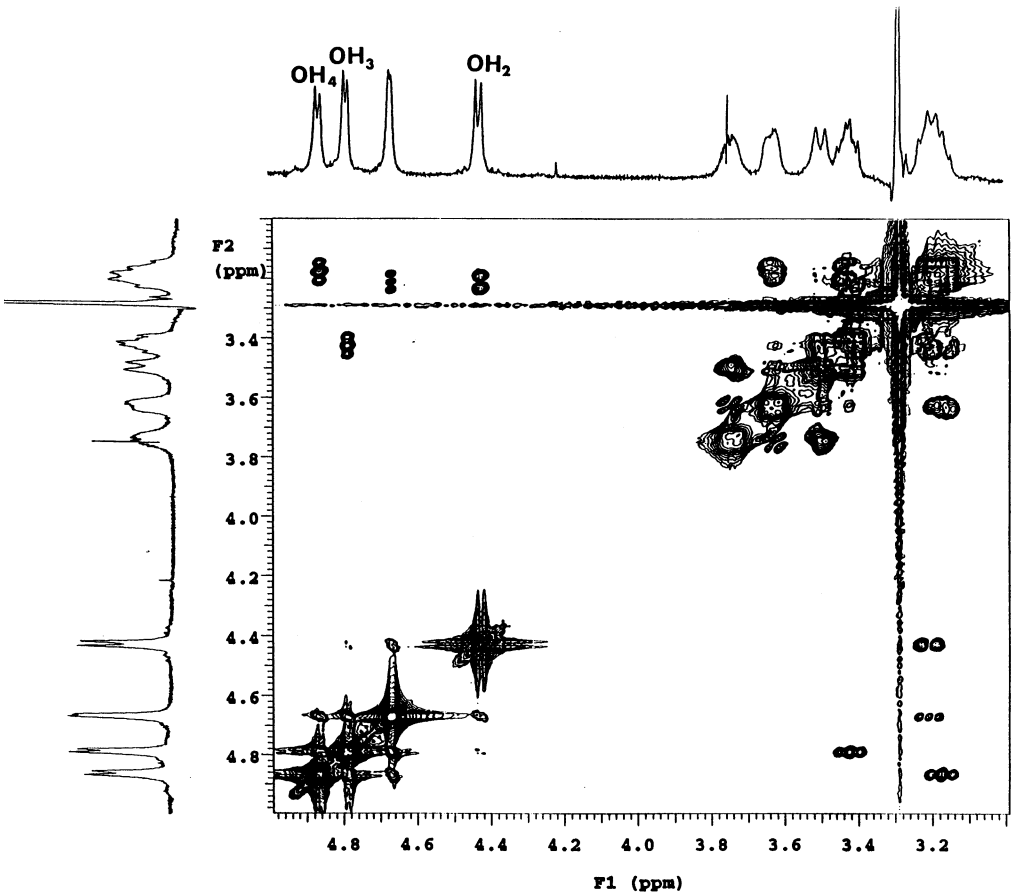

Fig. 5. Gradient H, H-COSY spectrum of dextran in Me_2SO-d_6 solutions at 30 °C.

the present analysis. Such models that are used to fit the experimental data of the hydroxymethyl carbon are the internal two-state jump model of London [58], and the restricted-amplitude internal diffusion model [59]. Both models have been used previously [30,31] to describe the hydroxyl internal motions of amylose and inulin.

The first model describes internal jumps between two stable states A and B, with lifetimes τ_A and τ_B. This motion of amplitude 2ξ (i.e., jumps in between $-\xi$ and $+\xi$), assumed to be independent, is superimposed on segmental motion that may be described by the HWH model. In the second model, O-6 moves continuously between two limiting values of an angle χ (i.e., the amplitude of restricted motion is 2χ). Restricted diffusion about a single axis has been solved analytically [59] and the resulting TCF can be combined with the TCF of the HWH model to give a new composite TCF, which incorporates the correlation time, τ_i, associated with internal motion. The composite TCFs for both models can be found in Ref. [30].

Both models were able to reproduce the NT_1 and NOE experimental data of the C-6 carbons of the two glucans. However, only the diffusion model was successful in reproducing

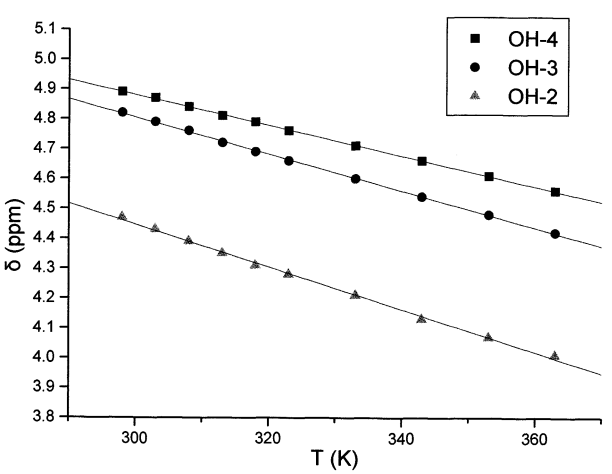

Fig. 6. Temperature dependence of the chemical shifts of the three hydroxyl protons of dextran in Me_2SO-d_6 solutions.

the experimental NT_2 data of the hydroxymethyl carbon of the β-(1→3)-D-glucans. Also, the restricted diffusion model is favored for two additional reasons. First, it requires fewer adjustable parameters than the two-state jump model in order to fit the data, and second, the fitting by the latter model resulted in physically unrealistic values of the correlation times, which did not follow an Arrhenius-type behavior.

Fig. 3(a–d) show plots of experimental data of the C-6 carbons of the two glucans and the best fit obtained by using the restricted diffusion model. Clearly, the agreement between the experimental and calculated values is very good. Table 2 summarizes the optimized parameters of the diffusion model. The correlation times, τ_i, are not very different for the two glucans. The Arrhenius plots of the correlation times, τ_i, gave comparable apparent activation energies of 18 and 14 kJ mol^{-1} for α-(1→3)-D-glucan, and β-(1→3)-D-glucan, respectively. Internal rotations are restricted in nature, characterized by amplitudes between 120–160° for both glucans in the temperature range of 100 °C. The similar range of the amplitude 2χ observed for these glucans indicates that the internal rotation of the hydroxymethyl group is equally restricted in the two polysaccharides.

It should be noted that the restricted diffusion model was not able to reproduce the relaxation data of the hydroxymethyl carbon of dextran in both Me_2SO and D_2O solvents. This carbon is situated on the backbone of the polysaccharide and relaxes via multiple internal motions about three bonds, namely the C-5–C-6 and C-6–O-1, and O-1–C-1 bonds. Therefore the DLM model was applied to describe the relaxation data of the backbone methylene C-6 carbon in these two solvents. The parameters of the DLM model in Table 2 obtained from the fitting of the ring carbons of dextran were able to reproduce the relaxation data of the C-6 carbon as shown in Fig. 3(e,f) in Me_2SO, and Fig. 3(g,h) in water.

Solvent dependence of the local dynamics.— In a previous paragraph, we compared the segmental dynamics of dextran in water and Me_2SO solvents. We divided the correlation time describing segmental motions by solvent viscosity, assuming tacitly that the correlation time τ_1 for conformational transitions is proportional to solvent viscosity. Also, Eq. (9), from which the barrier heights for conformational transitions were calculated, assumes that the experimental activation energy, E_a, is the sum of the barrier height for conformational transitions, E^*, and the activation energy, E_η, for the viscous flow. These assumptions are the basis of Kramers theory [49], which predicts that the rate constant for conformational transition is proportional to the solvent viscosity:

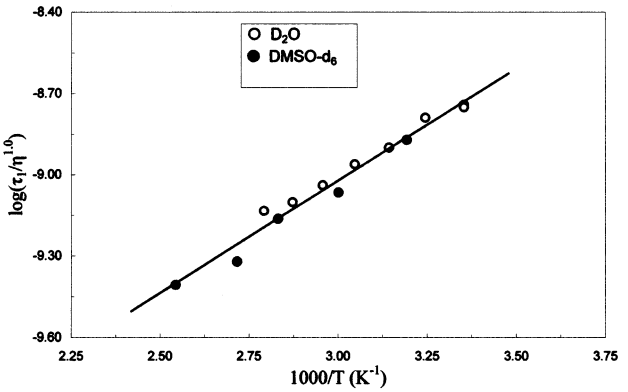

Fig. 7. Temperature dependence of the reduced correlation time ($\tau_1/\eta^{1.0}$) for chain segmental motion of dextran vs $1/T$ (K^{-1}) (Eq. (10)) in Me_2SO-d_6, and D_2O solutions. Filled symbols, data in Me_2SO-d_6; open symbols, data in D_2O.

$$\tau_1 = A\eta^{1.0} \exp(E^*/RT) \quad (10)$$

E^* is a property of the polymer only. Eq. (10) predicts that a plot of log τ_1 vs log η should be linear with unity slope. Such a procedure requires relaxation experiments in several solvents, which cannot be realized for the present polysaccharides due to their limited solubility in many organic solvents. Nevertheless, the applicability of Kramers theory can be tested in another way, that is, by scaling the correlation time with solvent viscosity. Fig. 7 shows a plot of log ($\tau_1/\eta^{1.0}$) vs $1/T$ for dextran; τ_1 values are taken from Table 2. The linear plot in Fig. 7 indicates that Kramers theory is correct for this polysaccharide in these two solvents. The value of E^* obtained from the best fit slope through the points of the plot in Fig. 7 is 15.6 ± 2.5 kJ mol^{-1}. This value compares favorably with the values obtained from Eq. (9), and implies that the observed potential energy E^* is independent of the solvent viscosity.

Temperature–frequency superposition.— Guillermo et al. [60] have described a method to superpose NT_1 data measured at different Larmor frequencies. A perfect superposition would result if all the time constants, τ_C, that enter into the explicit expression of the TCF have the same temperature dependence. This means that the shape of $G(t)$ is independent of temperature. Since NMR T_1 measurements are only sensitive to motions on time scales near the inverse of the Larmor frequency, a sufficient condition for superposition is that relaxation times near the inverse of the Larmor frequency ($1/\omega_C$) should have the same temperature dependence. Therefore, a plot of $\log(NT_1/\omega_C)$ vs $\log[\omega_C\tau_C(T)]$ should result in a single master curve. This temperature–frequency superposition has been tested on many synthetic polymers [34,42,43,61,62], and the polysaccharides amylose and inulin [31]. Fig. 8(a,b) shows plots of $\log(NT_1/\omega_C)$ vs $\log[\omega_C\tau_1(T)]$ for the α-(1→3)-D-glucan and β-(1→3)-D-glucan, respectively, τ_1 being the correlation time for segmental motions associated with the DLM model (Table 2). These plots reflect the frequency–temperature superposition of the NT_1 data of the two polysaccharides collected at different Larmor frequencies. Data from two and three Larmor frequencies superpose very well over the entire temperature range. The success of such a superposition demonstrates that all motional time constants contributing to spin relaxation are proportional to $\tau_1(T)$ and justifies attempts to fit the data to the TCF of the DLM model.

However, a more subtle question can be raised regarding the shape of the TCF in different solvents. Does the solvent identity play a role in the shape of the TCF? The plot in Fig. 8(c) tests the shape of the correlation function in Me_2SO and water solvents. The success of the superposition of the data from three magnetic field and two different solvents indicates that the DLM function has the same shape in these two solvents.

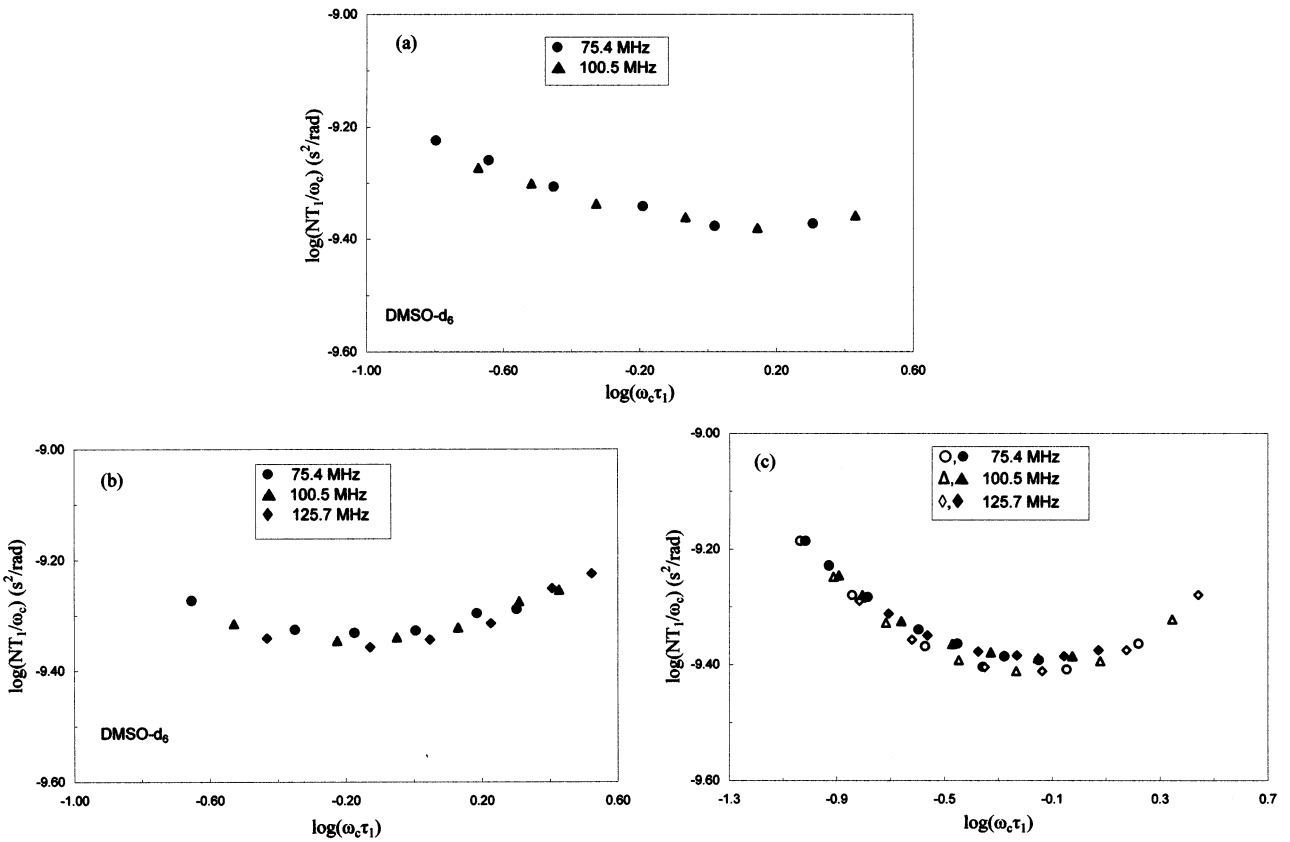

Fig. 8. Frequency–temperature superposition of the ^{13}C NMR NT_1 values for the ring carbons of (a) α-(1→3)-D-glucan, (b) β-(1→3)-D-glucan in Me_2SO-d_6 solutions, (c) dextran in Me_2SO-d_6, and in D_2O solutions. Filled symbols, data in Me_2SO-d_6; open symbols, data in D_2O.

Comparison of the dynamics of five polysaccharides.—Table 2 contains the simulation parameters of the DLM model for five polysaccharides that differ in the type of linkage and/or the nature of the monomer unit. The parameters for amylose and inulin have been taken from previous work [31]. The following observations can be made: (1) the τ_1 values, when adjusted for the difference in solvent viscosity (assuming that Kramers theory is valid), indicate that the segmental motion of these biopolymers decreases according to the order; inulin > dextran > α-(1→3)-D-glucan > β-(1→3)-D-glucan ~ amylose. This trend in flexibility of the carbohydrate chain appears to be in good agreement with theoretical [8,9,22,63–66] and experimental data [67–71] regarding the chain conformation and chain configuration of the present polysaccharides. Amylose behaves as a random coil with short, loosely wound, helical segments. Helical persistence is perceptible for β-(1→3)-D-glucan, whereas α-D-(1→3)-glucan behaves as a random coil lacking helical segments [8,64,66]. Moreover, the skeletal conformational freedom of amylose and β-(1→3)-D-glucan is smaller than that of α-(1→3)-D-glucan owing to the more constrained conformational energy surface calculated for the former polysaccharides. For dextran, the third chemical bond in the linkage region ensures greater separation of the pyranose rings, and hence reduces steric restrictions to rotation about the linkage bond [22,64,66]. Dextran does not have a particular favored conformation, and behaves as a random coil polymer [22,64,66,71].

The scarcity of experimental data of polysaccharides in Me_2SO solutions does not allow a comparison of the conformational behavior of the present polysaccharides. Recently, on the basis of solution studies on amylose in Me_2SO, it has been proposed [69] that the global conformations of high molecular weight amylose in Me_2SO and water are essentially the same, that is, the amylosic chain behaves as a random coil polymer with some helical nature. (2) The energetics of the segmental motions of all polysaccharides is reflected in the E^* values obtained from Eq. (9), that is, 9 kJ mol^{-1} for amylose, 10 kJ mol^{-1} for inulin, 15 and 16 kJ mol^{-1} for dextran in Me_2SO-d_6 and D_2O solutions, respectively, 14.5 kJ mol^{-1} for α-(1→3)-D-glucan, and 9 kJ mol^{-1} for β-(1→3)-D-glucan in Me_2SO-d_6 solutions. (3) The local dynamics depends on the particular geometry of the polysaccharide chain and/or the existence of intramolecular hydrogen bonding. This observation is reflected in the θ values of the librational motion of the C–H vector of the C-4 carbon of dextran in D_2O solutions. The librational motions in amylose and inulin have been discussed in detail in Ref. [31]. (4) Internal rotations of the hydroxymethyl groups are restricted in nature, characterized by amplitudes, 2χ, between 120 and 270° for inulin, 80 and 120° for amylose, and 120 and 160° for α-(1→3)-D-, and β-(1→3)-D-glucans. This range of the 2χ values, and the calculated rates of the restricted diffusion motion around the C-5–C-6 bond, indicate that the restriction of the internal rotation of the exocyclic hydroxymethyl groups of these polysaccharides decreases in the order; inulin > α-(1→3)-D-glucan ~ β-(1→3)-D-glucan > amylose. (5) A collective measure of cooperativity involving chain segments of various lengths is reflected on the ratio τ_0/τ_1 of the DLM model (Table 2). These values indicate that inulin ($\tau_0/\tau_1 = 2$) in water, dextran ($\tau_0/\tau_1 = 3$), and α-(1→3)-D-glucan ($\tau_0/\tau_1 = 3$) in Me_2SO are characterized by a small cooperativity range involving two to three monomer units, whereas segmental motion is localized within a larger length scale for dextran in water ($\tau_0/\tau_1 = 8$), β-(1→3)-D-glucan ($\tau_0/\tau_1 = 5$), and amylose ($\tau_0/\tau_1 = 7$) in Me_2SO.

4. Conclusions

The present study attempts to describe the backbone rearrangement and the internal motions of the exocyclic hydroxymethyl groups of the linear polysaccharides dextran, α-(1→3)-D-glucan, and β-(1→3)-D-glucan in water and Me_2SO solutions. The DLM model and the restricted diffusion model appear to be a reasonable basis for the present analysis of the relaxation data.

Comparison of the simulation parameters of these two models for the aforementioned

polysaccharides with those for amylose and inulin obtained from a previous study [31] showed a number of interesting features that reflect differences in the local geometries of these carbohydrate chains. However, it should be mentioned that the DLM model describes single and cooperative transitions in synthetic polymer chains in the form of trans–gauche isomerizations. Cooperative motions do occur in a carbohydrate chain as showed by Brant and co-workers [21,22]. Conformational transitions in a carbohydrate chain are not completely isolated events. However, the nature and the extent of these cooperative motions in a carbohydrate chain should differ from those occurring in a hydrocarbon chain. One way may be coupled torsional motions, that is, groups of torsions around the glycosidic bonds that can move cooperatively, so that small angular motions in many individual torsions add up to a large C–H vector of reorientation.

Librational motions of the internuclear C–H vectors, which are described by the DLM model, are believed to play an important role in the short time dynamics of synthetic polymer chains [34]. In contrast to conformational transitions, which occur by overriding potential wells, librational motions occur within potential wells and reach their equilibrium distribution before a significant number of conformational transitions occur.

What is the nature of these potential wells for the librational motions of the C–H vectors situated on a glucopyranosyl or a glucofuranosyl residue of a polysaccharide chain? The general theoretical treatment of conformation of polysaccharides assumes that the five- or six-membered rings are rigid moieties and adopt their minimum energy conformation. These treatments consider that the distortions of the valence lengths and angles from their equilibrium values have relatively small thermal amplitude in order to affect molecular conformation significantly. This assumption facilitates the calculation of conformation-dependent properties of polysaccharide chains. Nevertheless, pseudorotation in furanose residues [72] may render this assumption inappropriate. Moreover, as noted by Brant and Goebel [9], vibrational modes of the pyranose ring in the chair conformation can distort the ring through coupled displacements of the endocyclic valence and torsion angles from their equilibrium values. These distortions can be of relatively large amplitudes as concluded from infrared and Raman spectra [73]. A more serious piece of evidence regarding the existence of such motions comes from a recent NMR and MD study [74] on simple monosaccharide molecules. It was found that all ring carbons in all sugars studied exhibited a similar disorder that could arise from ring deformations in the form of ring librations. In particular, angular distribution trajectories obtained from MD simulations, and moments analysis of angle distribution for α-glucopyranose showed explicitly the occurrence of ring deformations from an ideal $^4C_1$ chair conformation [74]. Although ring deformations of monomer residues of a polysaccharide chain are expected to be less severe as compared to those for simple saccharides, it may be concluded that librational motions of C–H vectors occur in polysaccharides. This short time dynamics requires an extensive theoretical investigation, in terms of the evolution of the distribution of distortions of the valence and torsion angles in a sugar residue.

The potential barriers for the segmental motions obtained for the α-(1→3)-D-glucan and in particular for the α-(1→6)-D-glucan chains are greater than those observed for the α-(1→4)-D- and β-(1→3)-D-glucans. This observation is surprising, since the former polysaccharides are more flexible than the latter, and therefore their segmental motions should occur by overriding lower potential barriers. Apparently the potential barrier derived from the DLM model does not describe the trajectory of the segmental motions along the energy surface with the least potential energy, but it is rather sensitive to the overall shape of the potential energy surface. In this respect, the E^* values represent a statistical average of potential energies for all allowed conformations of each polysaccharide in terms of the torsional angles φ and ψ (and ω for dextran) about the glycosidic bonds. Conformational energy calculations for the dimeric analogues of the present polysaccharides showed [22,64,66] that the conforma-

tional space of the allowed conformations for α-(1→6)-D-glucopyranose, and to a lesser extent that for α-(1→3)-D-glucopyranose, are larger than those calculated for α-(1→4)-D- and β-(1→3)-D-glucopyranose. This indicates that the higher E^* values for the segmental motions of the former polysaccharides are associated with a larger collection of allowed conformations with potential energies as high as 40 kJ mol^{-1} above the global minimum.

A more rigorous treatment of segmental dynamics in carbohydrate chains requires a theory that employs some kind of reduced statistical analysis of the structural details of the carbohydrate chain in order to construct low energy chain trajectories. Such a theory has been developed recently by Perico and co-workers [75] on the basis of the optimum Rouse–Zim approximation (ORZ) to the generalized Langevin diffusion equation in the full configurational space. This theory, the so-called optimum Rouse–Zim for local dynamics (ORZLD), involves a structural matrix which contains all the conformational details of the polymer system. This matrix can be obtained from the full conformational energy map of the chain and subsequent Monte Carlo calculations. Thus, the ORZLD model provides the actual form of the TCF required to interpret the NMR relaxation data in terms of the specific geometry of a carbohydrate chain.

Acknowledgements

The authors gratefully acknowledge financial support from NATO (Grant No. CRG 9600593). Financial support from the University of Crete and the General Secretariat for Research and Technology is appreciated. The authors thank Professor A. Cesaro of the University of Trieste for helpful discussions.

References

[1] M. Yalpani, *Polysaccharides, Syntheses, Modifications and Structure/Property Relations*, Elsevier, Amsterdam, 1988.
[2] (a) N. Sharon, H. Lis, *Science*, 246 (1989) 227–234. (b) N. Sharon, H. Lis, *Sci. Am.*, (1993) 74–81.
[3] K. Drickamer, J. Carver, *Curr. Opin. Struct. Biol.*, 2 (1992) 653–654.
[4] D.A. Rees, W.E. Scott, *J. Chem. Soc. B*, (1971) 469–479.
[5] T.L. Bluhm, A. Sarko, *Carbohydr. Res.*, 54 (1977) 125–138.
[6] B.K. Sathyanarayana, V.S.R. Rao, *Biopolymers*, 10 (1971) 1605–1615.
[7] B.K. Sathyanarayana, V.S.R. Rao, *Biopolymers*, 11 (1972) 1379–1394.
[8] B.A. Burton, D.A. Brant, *Biopolymers*, 22 (1983) 1769–1792.
[9] D.A. Brant, K.D. Goebel, *Macromolecules*, 8 (1975) 522–530.
[10] B.K. Sathyanarayana, E.S. Stevens, *J. Biomol. Struct. Dyn.*, 1 (1983) 947–952.
[11] B.K. Sathyanarayana, E.S. Stevens, *J. Biomol. Struct. Dyn.*, 2 (1984) 443–448.
[12] D.A. Brant, M.D. Christ, Computer modeling of carbohydrate molecules, in A.D. French, J.W. Brady (Eds.), *ACS Symposium 430*, American Chemical Society, Washington, 1990, pp. 42–68.
[13] K. Ogawa, K. Okamura, A. Sarko, *Int. J. Biol. Macromol.*, 3 (1981) 31–36.
[14] K. Ogawa, T. Yui, K. Okamura, A. Misaki, *Biosci. Biotech. Biochem.*, 58 (1994) 1326–1327.
[15] Y. Deslandes, R.H. Marchessault, *Macromolecules*, 13 (1980) 1466–1471.
[16] W.T. Winter, A. Sarko, *Biopolymers*, 13 (1974) 1461–1482.
[17] M. Hricovini, R.N. Shah, J.P. Carver, *Biochemistry*, 31 (1992) 10018–10023.
[18] M. Hricovini, G. Torri, *Carbohydr. Res.*, 268 (1995) 159–175.
[19] D.A. Cumming, J.P. Carver, *Biochemistry*, 26 (1987) 6676–6683.
[20] D.A. Cumming, J.P. Carver, *Biochemistry*, 26 (1987) 6664–6676.
[21] M. Kadkhodael, H. Wu, D.A. Brant, *Biopolymers*, 31 (1991) 1581–1592.
[22] D.A. Brant, H.-S. Liu, Z.S. Zhu, *Carbohydr. Res.*, 278 (1995) 11–26.
[23] P. Dais, *Adv. Carbohydr. Chem. Biochem.*, 51 (1995) 63–131.
[24] A.S. Perlin, B. Casu, in G.O. Aspinall (Ed.), *The Polysaccharides*, Academic Press, New York, 1982, Vol. 1, Ch. 4.
[25] P.A.J. Gorin, *Adv. Carbohydr. Chem. Biochem.*, 38 (1981) 13–104.
[26] F.R. Seymour, R.D. Knapp, *Carbohydr. Res.*, 81 (1980) 67–103.
[27] K. Matsuo, *Macromolecules*, 17 (1984) 449–452.
[28] P. Dais, *Macromolecules*, 18 (1985) 1351–1354.
[29] P. Dais, *Carbohydr. Res.*, 160 (1987) 73–93.
[30] P. Dais, R.H. Marchessault, *Macromolecules*, 24 (1991) 4611–4614.
[31] E. Tylianakis, P. Dais, I. Andre, F.R. Taravel, *Macromolecules*, 28 (1995) 7962–7966.
[32] L. Catoire, C. Derouet, A.-M. Redon, R. Goldberg, C. Herve du Penhoat, *Carbohydr. Res.*, 300 (1997) 19–29.
[33] R.R. Ernst, *J. Chem. Phys.*, 45 (1966) 3845–3861.
[34] P. Dais, A. Spyros, *Progr. NMR Spectrosc.*, 27 (1995) 555–633.
[35] F. Heatley, *Progr. NMR Spectrosc.*, 13 (1979) 47–85.
[36] For a review of gradient H, H-COSY and HSQC experiments see: S. Braun, H.-O. Kalinowski, S. Berger, *100 and more Basic NMR Experiments. A Practical Course*, VCH, Weinheim, 1996.
[37] D.J. Craik, A. Kumar, G.C. Levy, *J. Chem. Int. Comput. Sci.*, 1 (1983) 30–38.

[38] A. Isiahara, *Adv. Polym. Sci.*, 5 (1968) 531–567.
[39] R.P. Lubianez, A.A. Jones, M. Bisceglia, *Macromolecules*, 12 (1979) 1141–1145.
[40] J.D. Gutnell, J.A. Glasel, *J. Am. Chem. Soc.*, 99 (1977) 42–43.
[41] D. Doddrell, V. Glushko, A. Allerhand, *J. Chem. Phys.*, 56 (1972) 3683–3689.
[42] D.J. Gisser, S. Glowinowski, M.D. Ediger, *Macromolecules*, 24 (1991) 4270–4277.
[43] W. Zhu, M.D. Ediger, *J. Polym. Sci., Polym. Phys. Ed.*, 35 (1997) 1241–1250.
[44] R. Dejean de la Batie, F. Laupretre, L. Monnerie, *Macromolecules*, 21 (1988) 2045–2052.
[45] J. Schafer, *Macromolecules*, 6 (1972) 882–888.
[46] (a) C.K. Hall, E. Helfand, *J. Chem. Phys.*, 77 (1982) 3275–3282. (b) T.A. Weber, E. Helfand, *J. Phys. Chem.*, 87 (1983) 2881–2889.
[47] A.A. Jones, W.H. Stockmayer, *J. Polym. Sci., Polym. Phys. Ed.*, 15 (1977) 847–861.
[48] O.W. Howarth, *J. Chem. Soc., Faraday Trans.*, 75 (1980) 1031–1041.
[49] H.A. Kramers, *Physica*, 7 (1940) 284–304.
[50] C. Guizard, H. Chanzy, A. Sarko, *J. Mol. Biol.*, 183 (1985) 397–408.
[51] S. Pérez, *Methods Enzymol.*, 203 (1991) 510–556.
[52] M. St-Jacques, P.R. Sundararajan, K.J. Taylor, R.H. Marchessault, *J. Am. Chem. Soc.*, 98 (1976) 4386–4391.
[53] P. Dais, A.S. Perlin, *Carbohydr. Res.*, 169 (1987) 159–169.
[54] K. Bock, R.U. Lemieux, *Carbohydr. Res.*, 100 (1982) 63–74.
[55] P.A.J. Gorin, *Adv. Carbohydr. Chem. Biochem.*, 38 (1981) 13–104.
[56] A. Spyros, P. Dais, *Macromolecules*, 25 (1992) 1062–1067.
[57] D.E. Woessner, *J. Chem. Phys.*, 31 (1962) 647–654.
[58] R.E. London, *J. Am. Chem. Soc.*, 100 (1978) 2678–2685.
[59] R.E. London, J.A. Avitabile, *J. Am. Chem. Soc.*, 100 (1978) 7159–7165.
[60] A. Guillermo, R. Dupeyre, J.P. Cohen-Addad, *Macromolecules*, 23 (1990) 1291–1297.
[61] E. Tylianakis, P. Dais, F. Heatley, *J. Polym. Sci. Part B: Polym. Phys.*, 35 (1997) 317–329.
[62] W. Zhu, M.D. Ediger, *Macromolecules*, 28 (1995) 7549–7557.
[63] (a) D.A. Brant, W.L. Dimpfl, *Macromolecules*, 3 (1970) 655–664. (b) K.D. Goebel, W.L. Dimpfl, D.A. Brant, *Macromolecules*, 3 (1970) 644–654. (c) R.C. Jordan, D.A. Brant, A. Cesaro, *Biopolymers*, 17 (1978) 2617–2632.
[64] D.A. Brant, *Pure Appl. Chem.*, 69 (1997) 1885–1892 and references therein.
[65] V.S.R. Rao, N. Yathindra, P.R. Sundararajan, *Biopolymers*, 8 (1969) 325–333.
[66] E. Tylianakis, A. Perico, A. Cesaro, P. Dais, *Carbohydr. Res.*, submitted for publcation
[67] (a) H. Elmgren, *Biopolymers*, 23 (1984) 2525–2541. (b) B. Ebert, H. Elmgren, *Biopolymers*, 23 (1984) 2543–2557. (c) H. Elmgren, *Carbohydr. Res.*, 160 (1987) 227–241.
[68] R.L. Whistler, J.R. Daniel, in R.L. Whistler, J.N. BeMiller, E.F. Panschall, (Eds.), *Starch Chemistry and Technology*, 2nd ed., Academic Press, New York, 1984, Ch. 6.
[69] Y. Nakanishi, T. Norisuye, A. Teramoto, *Macromolecules*, 26 (1993) 4220–4225.
[70] (a) I. Hirano, Y. Einaga, H. Fujita, *Polym. J.*, 11 (1979) 901–904. (b) Y. Adachi, N. Ohno, T. Yadomae, *Carbohydr. Res.*, 198 (1990) 11–122.
[71] A.M. Basedow, K.H. Ebert, *J. Polym. Sci., Polym. Symp.*, 66 (1979) 101–115.
[72] J.F. Stoddart, *Stereochemistry of Carbohydrates*, Interscience, New York, 1971.
[73] (a) H.M. Pickett, H.L. Strauss, *J. Chem. Phys.*, 53 (1970) 276–281. (b) H.M. Pickett, H.L. Strauss, *J. Am. Chem. Soc.*, 92 (1970) 7281–7290. (c) H.L. Strauss, *J. Chem. Educ.*, 48 (1971) 221–223.
[74] P.J. Hajduk, D.A. Horita, L.E. Lerner, *J. Am. Chem. Soc.*, 115 (1993) 9196–9201.
[75] (a) A. Perico, *Acc. Chem. Res.*, 22 (1989) 336–342. (b) A. Perico, *Biopolymers*, 28 (1989) 1527–1540 and refs. therein.